Evolution of Negative Cooperativity in Glutathione Transferase Enabled Preservation of Enzyme Function

Alessio Bocedi, Raffaele Fabrini, Mario Lo Bello, Anna Caccuri, Giorgio Federici, Bengt Mannervik, Athel Cornish-Bowden, Giorgio Ricci

THE JOURNAL OF BIOLOGICAL CHEMISTRY VOL. 291, NO. 52, pp. 26739–26749, December 23, 2016

Evolution of Negative Cooperativity in Glutathione Transferase Enabled Preservation of Enzyme Function*

Received for publication, July 20, 2016, and in revised form, November 3, 2016 Published, JBC Papers in Press, November 4, 2016, DOI 10.1074/jbc.M116.749507

Alessio Bocedi[‡], Raffaele Fabrini[‡], Mario Lo Bello[§], Anna Maria Caccuri[¶], Giorgio Federici[‡], Bengt Mannervik[‖], Athel Cornish-Bowden[**], and Giorgio Ricci[‡1]

From the [‡]Department of Chemical Sciences and Technologies, [§]Department of Biology, and [¶]Department of Experimental Medicine and Surgery, University of Rome, Tor Vergata, Rome 00133, Italy, [‖]Department of Neurochemistry, Stockholm University SE-10691 Stockholm, Sweden, and [**]Aix Marseille Université, CNRS, Bioénergétique et Ingénierie des Protéines, Institut de Microbiologie de la Méditerranée, 13009 Marseille, France

Edited by Norma Allewell

Negative cooperativity in enzyme reactions, in which the first event makes subsequent events less favorable, is sometimes well understood at the molecular level, but its physiological role has often been obscure. Negative cooperativity occurs in human glutathione transferase (GST) GSTP1-1 when it binds and neutralizes a toxic nitric oxide adduct, the dinitrosyl-diglutathionyl iron complex (DNDGIC). However, the generality of this behavior across the divergent GST family and its evolutionary significance were unclear. To investigate, we studied 16 different GSTs, revealing that negative cooperativity is present only in more recently evolved GSTs, indicating evolutionary drift in this direction. In some variants, Hill coefficients were close to 0.5, the highest degree of negative cooperativity commonly observed (although smaller values of n_H are theoretically possible). As DNDGIC is also a strong inhibitor of GSTs, we suggest negative cooperativity might have evolved to maintain a residual conjugating activity of GST against toxins even in the presence of high DNDGIC concentrations. Interestingly, two human isoenzymes that play a special protective role, safeguarding DNA from DNDGIC, display a classical half-of-the-sites interaction. Analysis of GST structures identified elements that could play a role in negative cooperativity in GSTs. Beside the well known lock-and-key and clasp motifs, other alternative structural interactions between subunits may be proposed for a few GSTs. Taken together, our findings suggest the evolution of self-preservation of enzyme function as a novel facility emerging from negative cooperativity.

Glutathione transferases are a superfamily of enzymes responsible for the metabolism and inactivation of a broad range of carcinogens and xenobiotics (1, 2). They catalyze the conjugation of glutathione (GSH) to many toxic organic compounds provided with an electrophilic center. They are also able to act as ligandins, binding and sequestering many types of toxins without any chemical reaction involved. This non-catalytic role has an important physiological impact because these proteins are abundantly expressed in all organisms, from bacteria to humans, approaching concentrations close to 1 mM in some cells (3). Cytosolic GSTs have been grouped into 13 gene-independent classes based upon their primary structure (4). An alternative classification is possible on the basis of the residue that in the active site (the G-site) favors the activation of GSH: the Cys-GSTs (Omega and Beta classes) whose structures are close to the ancestral precursor of all GSTs, the Ser-GSTs (Delta, Theta, Zeta, and Phi classes, including also Nu-GST activated by a threonine), and the Tyr-GSTs (Alpha, Pi, Mu, and Sigma classes); this latter subfamily comprises the more recently evolved GSTs. Most of these variants are dimeric proteins composed of identical subunits. However, heterodimeric GSTs composed of different members from the same class also occur (5). For many years GSTs were considered non-cooperative enzymes based on hyperbolic binding curves of substrates (6), further supported by the kinetic independence of subunits in heterodimeric GSTs demonstrated with various substrates as well as inhibitors (7, 8). However, in 1995 the replacement of a critical cysteine (Cys-47) by site-directed mutagenesis of the human GSTP1-1 disclosed a hidden intersubunit communication made evident by marked positive homotropic behavior for GSH binding (9). A few years later, other single point mutations on the same variant (10–12) as well as on other GSTs (13–14) also revealed hidden cooperativity.

Intersubunit communication in native GSTP1-1 was indicated by modification with thiol reagents (15), and the crystal structure (16) provided strong evidence for negative cooperativity in the enzyme. A number of different chemical or physical inactivators provided further support for this interpretation (17). In the meantime, a few other GSTs revealed cooperative properties in a native status, namely the murine GSTA4–4 (18), the human GSTA1-1 (19), and the *Plasmodium falciparum* GST (20, 21). However, the human GSTP1-1 remained the most peculiar and striking case of cooperativity among all GSTs, showing positive cooperativity for GSH binding at temperatures above 35 °C and negative cooperativity below 25 °C (22).

A particularly interesting GST ligand is the dinitrosyl-diglutathionyl-iron complex (DNDGIC)[2] (Fig. 1*A*) formed sponta-

* This work was supported in part by the grant "Consolidate the Foundations," University of Rome "Tor Vergata" (E82F16000810005) and by a grant from the Swedish Research Council. The authors declare that they have no conflicts of interest with the contents of this article.

[1] To whom correspondence should be addressed: Dept. of Chemical Sciences and Technologies, University of Rome, "Tor Vergata" via della Ricerca Scientifica 1, 00133 Rome Italy. Tel.: 39-672594353; Fax: 39-0672594328; E-mail: riccig@uniroma2.it.

[2] The abbreviations used are: DNDGIC, dinitrosyl-diglutathionyl-iron complex; DNGIC, dinitrosyl-glutathionyl-iron-complex; CDNB, 1-chloro,2,4-dinitrobenzene.

neously when an excess of nitric oxide is produced in the cell (23). By sequestering free iron and NO, this complex may counteract both oxidative and nitrosylative stress. However, DNDGIC is toxic to the cell as indicated by the significant induction of the SOS DNA repair systems (24), activation of the oxidative shock response (soxA) gene, and the gene Sfia inhibiting cell division (25). Moreover, it irreversibly inactivates glutathione reductase, an enzyme necessary for maintaining the redox balance of the cell (26). A few GST variants have been found to act as efficient DNDGIC ligandin proteins, displaying astonishing affinities. In particular, the recently evolved Tyr-GSTs show K_D values ranging from 10^{-9} to 10^{-12} M (23) making this complex a prime intracellular ligand for these enzymes. X-ray diffraction data demonstrated that DNDGIC binds to the G-site with loss of one glutathione (Fig. 1*B*), replacing it with the residue contributing to the GSH activation, *i.e.* tyrosine, serine, or cysteine that complete the coordination shell of the ferrous ion (27). By testing 39 different GSTs, we also found that the Cys-GSTs, which are close to the ancestral GST protein, have thousands of times lower affinity for DNDGIC than the Tyr-GSTs and Ser-GSTs (23). Thus, protection of the cell against NO by means of GSTs was proposed to recently have been acquired during evolution. Interestingly, Cys-GSTs are the only known GSTs expressed by bacteria, and their low affinity for DNDGIC has been related to the sensitivity of these organisms to nitrosylative stress (23). Notwithstanding the beneficial effects of the DNDGIC sequestration by GSTs, a likely disadvantage is that these enzymes, when saturated reversibly by this complex, become catalytically inactive and lose their ability to conjugate GSH to many other toxins. How is it possible to reconcile these two opposite needs, *i.e.* bind DNDGIC too tightly enough to be not easily released and at the same time preserve an essential and sufficient conjugating activity? The development of negative cooperativity for DNDGIC binding in GSTs appears to be an advantageous solution.

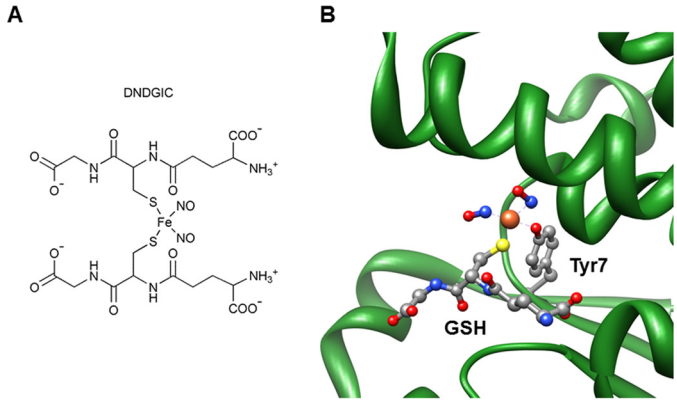

FIGURE 1. *A*, chemical structure of the dinitrosyl-diglutathionyl iron complex (DNDGIC). *B*, crystal structure of DNGIC bound to GSTP1-1 (one GSH is replaced by a Tyr residue, which completes the coordination shell of the iron ion with its -OH group). The structure is from PDB ID 1ZGN, the protein is in *green ribbons*, whereas DNGIC and Tyr-7 are depicted in *ball-and-stick* colored according to atom type (27).

This work shows that negative cooperativity is not restricted to GSTP1-1 but is present also in many other members of the GST superfamily never described as cooperative enzymes. We propose that negative cooperativity has evolved to maintain a residual conjugating activity of GST against toxins in the presence of DNDGIC. By this mechanism the physiological role of detoxication is safeguarded by a phenomenon, which may be reasonably defined as "cooperative self-preservation of function."

Results

DNDGIC Binding Triggers a Strong Negative Cooperativity in Many GSTs—In the present study 16 different GSTs, as representative members of the Tyr-, Ser-, and Cys-GST subfamilies, were examined in relation to their interaction with DNDGIC. Data reported in Table 1 show that almost all tested Tyr-GSTs and Ser-GSTs display a noticeable negative cooperativity for DNDGIC binding with Hill coefficients, $n_{H,}$ ranging from 0.51 to 0.75 (Table 1). If the adjacent subunit is still catalytically active in the half-saturated GSTs, this behavior would warrant a

TABLE 1

Cooperativity for DNDGIC binding in several GSTs

n_H are Hill coefficients, and K_{D1} and K_{D2} are dissociation constants for DNDGIC calculated by fluorometric experiments. Equations used for calculation of n_H and K_{D1} and K_{D2} are reported under "Experimental Procedures."

Glutathione transferase variants	n_H	K_{D1}	K_{D2}	K_{D2}/K_{D1}	Lock-and-key motif
Tyrosine subfamily[a]					
H. sapiens GSTP1-1	0.51 ± 0.06	1.5 ± 0.1	120 ± 5	80 ± 9	Yes
H. sapiens GSTA1-1	0.57 ± 0.06	0.08 ± 0.01	3.4 ± 0.1	43 ± 6	Yes
H. sapiens GSTA2-2	0.66 ± 0.06	0.20 ± 0.02	4.8 ± 0.2	24 ± 3	Yes
H. sapiens GSTA3-3	0.54 ± 0.05	0.07 ± 0.01	4.4 ± 0.1	63 ± 10	Yes
H. sapiens GSTM2-2	0.67 ± 0.07	1.2 ± 0.1	20 ± 2	17 ± 3	Yes
O. volvulus GST2	0.52 ± 0.05	6.4 ± 0.2	490 ± 20	77 ± 5	Yes
S. haematobium GST	0.65 ± 0.05	0.40 ± 0.02	10 ± 1	25 ± 4	Alternative
Serine subfamily[b]					
L. cuprina GSTc	1.0 ± 0.1	0.11 ± 0.01	0.11 ± 0.01[c]	1	No
A. dirus GSTD3-3	0.62 ± 0.06	0.14 ± 0.01	4.8 ± 0.3	34 ± 4	Yes (clasp)
A. dirus GSTD5-5	0.62 ± 0.06	0.11 ± 0.01	3.4 ± 0.1	31 ± 4	Yes (clasp)
A. dirus GSTD4-4	0.66 ± 0.05	0.22 ± 0.02	5.1 ± 0.3	23 ± 3	Yes (clasp)
H. sapiens GSTT2-2	0.75 ± 0.08	0.30 ± 0.02	3.9 ± 0.2	13 ± 2	Alternative
Cysteine subfamily[b]					
O. anthropic	0.95 ± 0.08	0.22 ± 0.03	0.22 ± 0.03[c]	1	No
B. xenovorans	1.0 ± 0.1	400 ± 20	400 ± 20[c]	1	No
S. paucimobilis	1.0 ± 0.1	60 ± 3	60 ± 3[c]	1	No
P. mirabilis	1.0 ± 0.1	350 ± 30	350 ± 30[c]	1	No

[a] Concentrations for K_{D1} and K_{D2} are measured in nM.
[b] Concentrations for K_{D1} and K_{D2} are measured in μM.
[c] For these GST variants the fits are essentially monophasic, and then the dissociation constants $K_{D1} = K_{D2}$.

residual conjugating activity even in the presence of a large amount of DNDGIC, *i.e.* in the case of relevant NO production in the cell. Notably, the Hill coefficients found for a few Tyr-GSTs approach the value of 0.5, which is the highest degree of negative cooperativity commonly observed in a dimeric enzyme (28). None of the GSTs taken as representative members of the Cys-GSTs subfamily shows any cooperativity (Table 1 and Fig. 2). Thus, these GSTs, all close to the ancestral precursor of GSTs, not only display 3 orders of magnitude lower affinity for DNDGIC than the Tyr- and Ser-GSTs but also lack any detectable intersubunit communication necessary for cooperative modulation. Interestingly, the average of both n_H and the ratio of the two apparent binding constants K_{D2}/K_{D1} for DNDGIC binding follow a trend that parallels the evolution pathway of these enzymes (Fig. 2). Representative fits of experimental data to the equations diagnostic for cooperativity are reported in Figs. 3, 4, and 5.

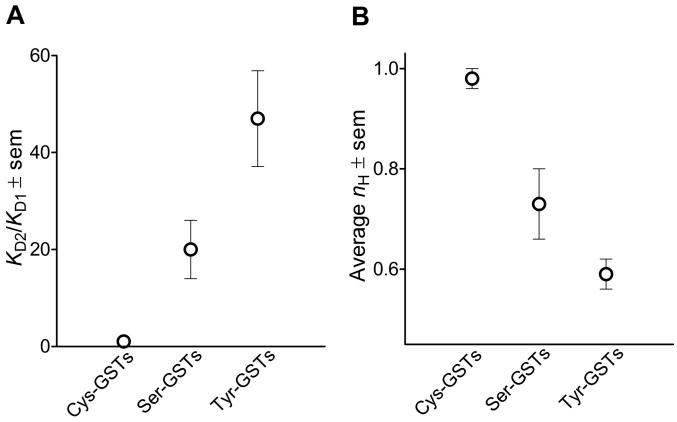

FIGURE 2. **Negative cooperativity for DNDGIC binding.** *A*, average (and S.E.) of the ratio between the two dissociation constants for GST-DNDGIC interaction (K_{D2}/K_{D1}) calculated for all tested dimeric GSTs (see Table 1) and grouped into the three sub-families. *B*, average (and S.E.) of all Hill coefficients calculated for all GSTs grouped into the three sub-families. Experimental details are reported under "Experimental Procedures."

The Negative Cooperativity Preserves the Enzymatic Activity in the Adjacent Subunit—By evaluating the effect of the cooperative binding of DNDGIC on the classical GST activity, *i.e.* its ability to conjugate GSH to 1-chloro-2,4-dinitrobenzene (CDNB), it is evident that many tested GSTs belonging to the Tyr- and Ser- subfamilies efficiently protect the activity of the adjacent subunit after the first one has bound DNDGIC. This may be quantified by means of a "protection factor" ($K_{i2}/K_{i1} - 1$) obtained by kinetic data, which indicates to what extent one subunit becomes more resistant to inactivation by DNDGIC when the adjacent subunit has bound this compound (Fig. 6). Among all tested Tyr-GST variants, GSTP1-1 and *Onchocerca volvulus* GST show the highest protection factors, but even the human GSTM2-2 and GSTA2-2 display remarkable protection values (Fig. 6). Among the Ser-GST variants, GSTD3 and GSTD5 are those showing the most efficient self-protection, whereas this mechanism is absent in *Lucilia cuprina* GST (Table 2). Obviously, no protection is obtained in the Cys-GSTs, which do not display any cooperativity (Fig. 6 and Tables 1 and 2). Two apparently paradoxical exceptions

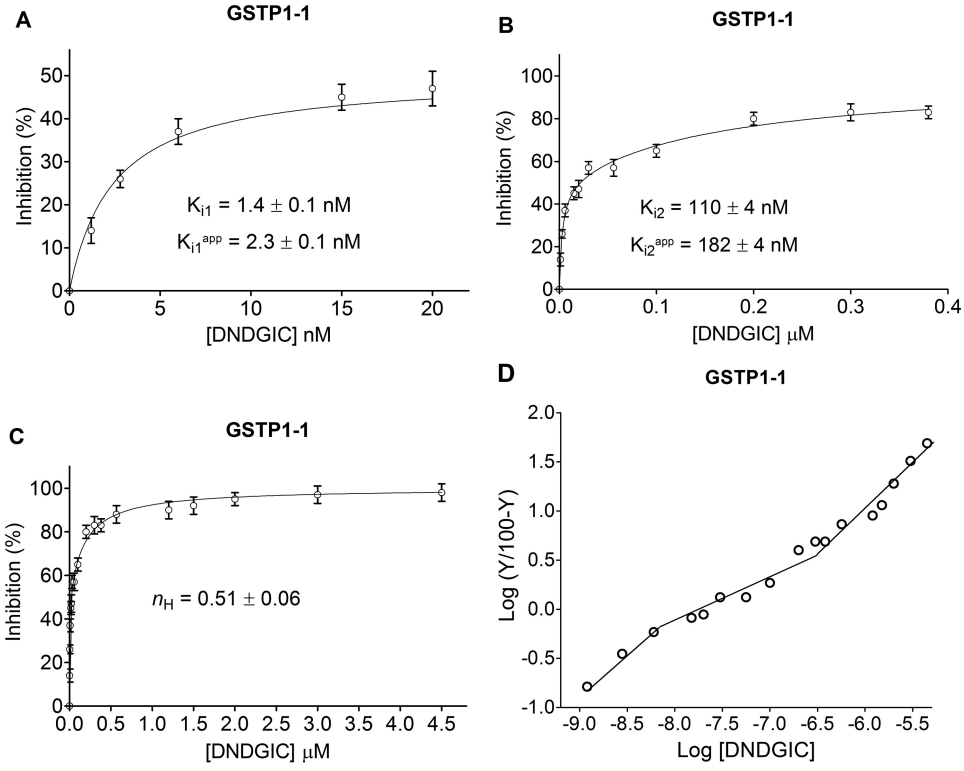

FIGURE 3. **Representative fits of inhibition data of GSTP1-1 (a cooperative GST).** Experimental inhibition data by DNDGIC were fitted by the two-site inhibition equation reported under "Experimental Procedures" to obtain K_{i1} and K_{i2} ($r^2 = 0.995$). *A*, section of the global fit showing the inhibition due to the binding of DNDGIC to the high affinity site. *B*, section of the global fit showing the inhibition due to the binding of DNDGIC to the low affinity site. Note that the plots show apparent K_i values (see Equation 1). *C*, experimental data for inhibition by DNDGIC, fitted to the Hill equation ($r^2 = 0.991$) reported under "Experimental Procedures," which provides n_H values. *Error bars* represent the S.D. *D*, Hill plot for the same experimental data reported in *panel C*. Coefficients of variation for each point do not exceed 12%.

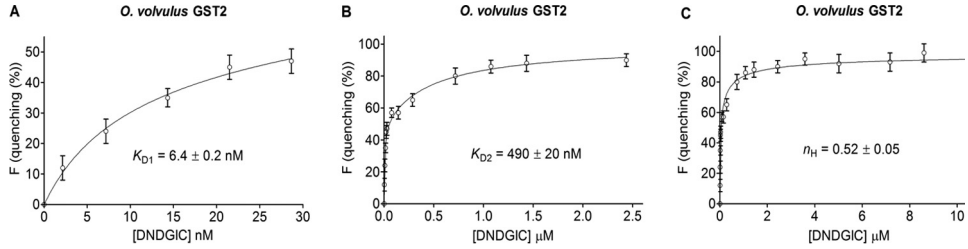

FIGURE 4. **Representative fits of the DNDGIC binding data to *O. volvulus* GST2 (a cooperative GST).** Experimental fluorescence quenching data by DNDGIC were fitted by the two-site binding equation reported under "Experimental Procedures" to obtain K_{D1} and K_{D2} ($r^2 = 0.994$). *A*, section of the fit showing the binding of DNDGIC to the high affinity site. *B*, section of the fit showing the binding of DNDGIC to the low affinity site. *C*, experimental inhibition data by DNDGIC fitted to the Hill equation ($r^2 = 0.990$) reported under "Experimental Procedures," which provides n_H values. *Error bars* represent the S.D.

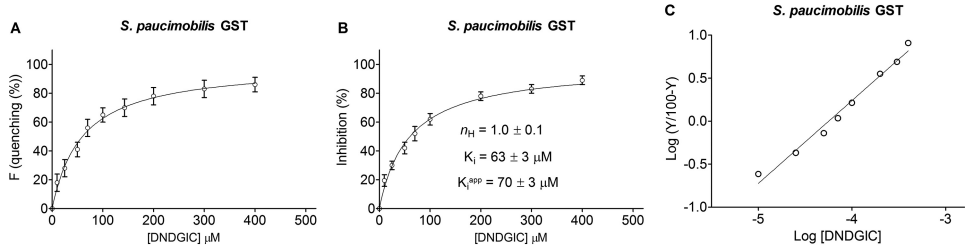

FIGURE 5. **Representative fits of the DNDGIC inhibition and binding data to *S. paucimobilis* GST (a non-cooperative GST).** Experimental fluorescence and inhibition data were fitted by the two-site binding and inhibition equations reported under "Experimental Procedures," obtaining $K_{D1} = K_{D2}$ and $K_{i1} = K_{i2}$. *A*, intrinsic fluorescence quenching of *S. paucimobilis* GST by DNDGIC ($r^2 = 0.993$). *B*, inhibition data by DNDGIC ($r^2 = 0.994$). The same inhibition data were also fitted by the Hill equation (plot not shown), giving the same curve as in *B* and an n_H value of 1.0 ± 0.1. *Error bars* represent the S.D. *C*, Hill plot for the same experimental data reported in *panel B*.

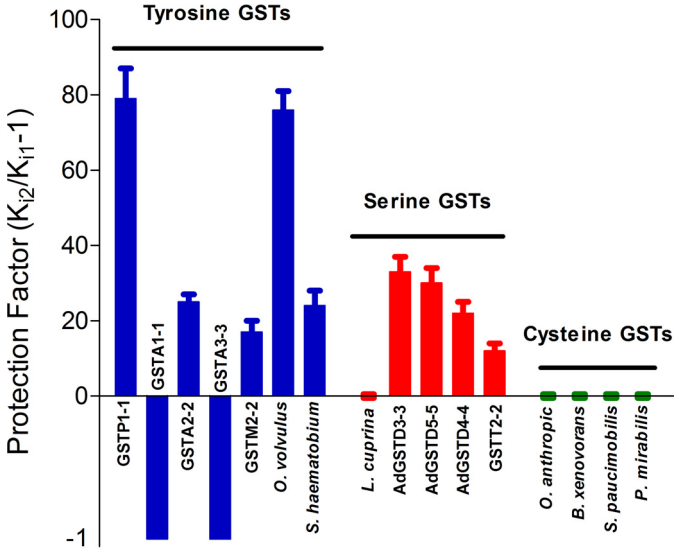

FIGURE 6. **Protection factors against inactivation due to DNDGIC binding.** Protection factor (by what factor does one subunit become more resistant to inactivation by DNDGIC when the adjacent subunit has bound this complex) is defined as ($K_{i2}/K_{i1} - 1$). The negative value (−1) for GSTA1-1 and GSTA3-3 (amplified in the plot) underlines an opposite phenomenon, *i.e.* a half-site inhibition where K_{i2} approaches zero. *Error bars* are derived from Table 2.

have been found, represented by GSTA1-1 and GSTA3-3 (Table 2), and their behavior will be explored more deeply below. Excluding these two variants, the average of K_{i2}/K_{i1} ratios produce similar values as calculated from the average of K_{D2}/K_{D1} ratios (coming from thermodynamic fluorescence data) for all the Tyr-GSTs and the Ser-GSTs (Tables 1 and 2). This coincidence occurs because binding of DNDGIC to one GST subunit leaves intact the catalytic efficiency of the adjacent subunit, as suggested by a residual activity in the half-saturated GSTs of ~50% of the original one. Actually, in the DNDGIC-half-saturated enzyme the affinity for GSH in the vacant subunit is not much changed. For example the half-saturated GSTP1-1 shows a $K_m = 0.22$ mM for GSH instead of 0.15 mM (data not shown). This increment does not modify the catalytic capacity of GSTs *in vivo* given that the GSH concentration in the cells is 1–8 mM. Fig. 7 explains the cooperative self-preservation mechanism found in GSTs. Even in the presence of DNDGIC in concentrations essentially saturating one subunit, the second subunit remains unliganded and catalytically active.

A Few Alpha Class GSTs Adopt a Half-of-the-sites Interaction—An interesting exception to the above described self-preservation found in the Tyr-GSTs and Ser-GSTs is represented by the Alpha class GSTA1-1 and GSTA3-3, both undergoing a typical half-of-the sites interaction, *i.e.* when one subunit binds DNDGIC, the adjacent one becomes fully inactive but still able to bind a second DNDGIC molecule with lower affinity (see Tables 1 and 2 and Fig. 6). This property, observed in the past for GSTA1-1 (29), is now also found for GSTA3-3, whereas the homologous GSTA2-2 follows the cooperative self-preservation behavior demonstrated for other GSTs. This finding is proved by plotting the residual activity of these GSTs as a function of substoichiometric additions of the inhibitor (Fig. 8, *A*–*C*). The peculiar affinities of these two variants toward DNDGIC and their expression and localization inside the cell suggest some possible comments. In fact, GSTA1-1 and GSTA3-3 display the highest affinity, showing 20 times higher affinity for DNDGIC ($\sim 8 \times 10^{-11}$ M) than all other Mu and Pi variants (1.5×10^{-9} M) (23). The complete loss of activity after the half-of-the-sites binding of DNDGIC seems to be the price that needs to be paid by these GSTs for assuming the role of interceptors toward DNDGIC. This suicide behavior inherent in their enzymatic activity is probably well tolerated by the cell, as the Alpha class GSTs are often co-expressed with a

TABLE 2

Inhibition constants for DNDGIC interaction with several GSTs

K_{i1} and K_{i2} are the true inhibition constants for DNDGIC calculated from the kinetics experiments via the apparent constants K_{i1}^{app} and K_{i2}^{app}. Equations used for calculation of K_{i1} and K_{i2} are reported under "Experimental Procedures."

Glutathione transferase variants	K_{i1}	K_{i2}	K_{i2}/K_{i1}	Self-preservation
Tyrosine subfamily[a]				
H. sapiens GSTP1-1	1.4 ± 0.1	110 ± 4	79 ± 8	Yes
H. sapiens GSTA1-1	0.07 ± 0.01	0[b]	0[b]	No
H. sapiens GSTA2-2	0.18 ± 0.01	4.6 ± 0.1	26 ± 2	Yes
H. sapiens GSTA3-3	0.05 ± 0.01	0[b]	0[b]	No
H. sapiens GSTM2-2	1.2 ± 0.1	22 ± 2	18 ± 3	Yes
O. volvulus GST2	6.5 ± 0.2	500 ± 20	77 ± 5	Yes
S. haematobium GST	0.44 ± 0.02	11 ± 1	25 ± 3	Yes
Serine subfamily[c]				
L. cuprina GSTc	0.10 ± 0.01	0.10 ± 0.01[d]	1	No
A. dirus GSTD3-3	0.15 ± 0.01	5.0 ± 0.3	33 ± 4	Yes
A. dirus GSTD5-5	0.12 ± 0.01	3.6 ± 0.1	30 ± 3	Yes
A. dirus GSTD4-4	0.24 ± 0.02	5.4 ± 0.3	23 ± 3	Yes
H. sapiens GSTT2-2	0.30 ± 0.02	4.0 ± 0.2	13 ± 2	Yes
Cysteine subfamily[c]				
O. anthropic	0.26 ± 0.03	0.26 ± 0.03[d]	1	No
B. xenovorans	440 ± 20	440 ± 20[d]	1	No
S. paucimobilis	63 ± 3	63 ± 3[d]	1	No
P. mirabilis	380 ± 30	380 ± 30[d]	1	No

[a] Concentrations for K_{i1} and K_{i2} are measured in nM.
[b] For GSTs that show half-of-the-site interaction the K_{i2} was assumed to be 0.
[c] Concentrations for K_{i1} and K_{i2} are measured in μM.
[d] For these GST variants the fits are essentially mono-phasic, then inhibition constants $K_{i1} = K_{i2}$.

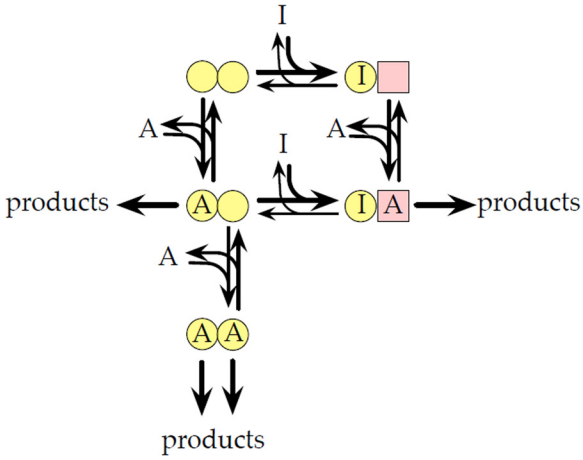

FIGURE 7. **The cooperative self-preservation mechanism found in GSTs as well as in other homo-dimeric enzymes.** *A* and *I* represent the substrate and the inhibitor, respectively. *Pink squares* represent the modified subunits, which do not bind (or scarcely interact with) the inhibitor molecule.

conspicuous level of Mu class GSTs, which show cooperative self-preservation and then guarantee a residual detoxifying activity toward other toxins in case of NO insults. Another safeguard is the presence of heterodimers containing a GSTA2 subunit, which could display activity when the other subunit binds DNDGIC. Graphic representation of the expression of all GSTs in human hepatocyte, their detoxifying capacity toward DNDGIC, and their conjugating activity toward toxic electrophilic compounds is given in Fig. 9, *A*, *B*, and *D*. It appears that all the defense capacity against DNDGIC in human hepatocytes is exclusively assumed by the Alpha GSTs, in particular by GSTA1-1 (Fig. 9*C*). The human GSTA3-3 is primarily expressed in steroidogenic tissues but not in liver (30); thus, its contribution in human hepatocytes to bind DNDGIC is null despite its strong affinity for this complex (Fig. 9).

A further important element that justifies the sacrifice of catalytic activity in the Alpha GSTs in favor of an acquired extraordinary affinity for DNDGIC is the peculiar cell localization of these variants. In fact, ~30% of the entire pool of Alpha-GSTs is concentrated near the inner and outer nuclear envelope, forming, as with many other enzymes, a defense barrier for DNA termed "nuclear shield" (31, 32). For this peculiar role, some Alpha GSTs developed an extraordinary affinity during evolution but, as it appears, at the expense of their catalytic efficiency.

Structural Requirements for Negative Cooperativity in GSTs—A classical structural explanation for negative or positive cooperativity is that one subunit, once it has bound a specific ligand, modifies the structure of the adjacent free subunit. The subunit interfaces, as they appear from the X-ray structures of many dimeric GSTs, help us to identify the structural requirements for the observed negative cooperativity. The two adjacent monomers display three types of interactions: polar contacts, hydrogen bonds, and hydrophobic interactions. For the mammalian Tyr-GSTs the combination of mutational, kinetic, and structural studies provide strong evidence for the structural basis of cooperativity, in particular for GSTP1-1 (33). By analogy, but with less experimental evidence, we suggest similar structural requirements for negative cooperativity in other GSTs below. In the Tyr-GSTs a typical hydrophobic contact, important for inter-subunit communication, is the "lock-and-key" motif. This structural trait is formed by an aromatic residue (key residue) from domain I in one subunit wedged into a hydrophobic pocket formed by helices 4 and 5 in domain II of the other subunit (lock apparatus) (Fig. 10*A*). The lock-and-key motif is a common feature of Pi, Mu, and Alpha class GSTs where the key residue is either phenylalanine or tyrosine (Tyr-49 or Tyr-50 with Met-1 residue in *h*GSTP1-1) buried in a hydrophobic pocket formed by Met-91, Val-92, Gly-95, Pro-128, Phe-129, and Leu-132 of the second subunit chain (Fig. 10*A*). Mutagenesis has been used to investigate the importance of the key residue for dimerization, stability, and cooperativity found in GSTP1-1 (34), GSTA1-1 (35), and GSTM1-1 (36). The

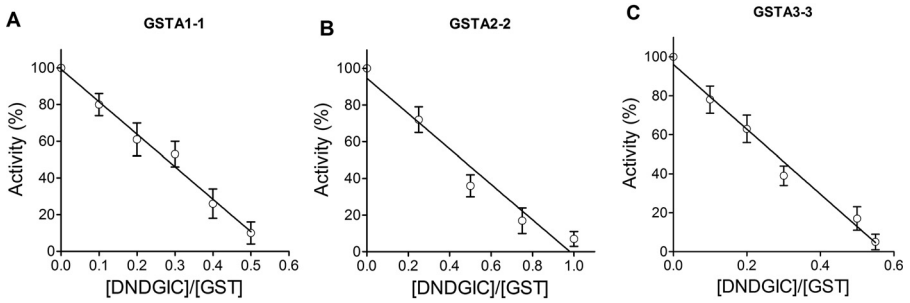

FIGURE 8. **Cooperative half-of-the sites inactivation and cooperative self-preservation in Alpha class GSTs.** Variable amounts of DNDGIC (from 0.4 to 4 μM) were incubated with 4 μM Alpha class GSTs in 0.1 M potassium phosphate buffer, pH 7.4 (*Panel A*, GSTA1-1; *Panel B*, GSTA2-2; *Panel C*, GSTA3-3). After 2 min of incubation, aliquots were assayed for GST activity. *Error bars* are S.D.

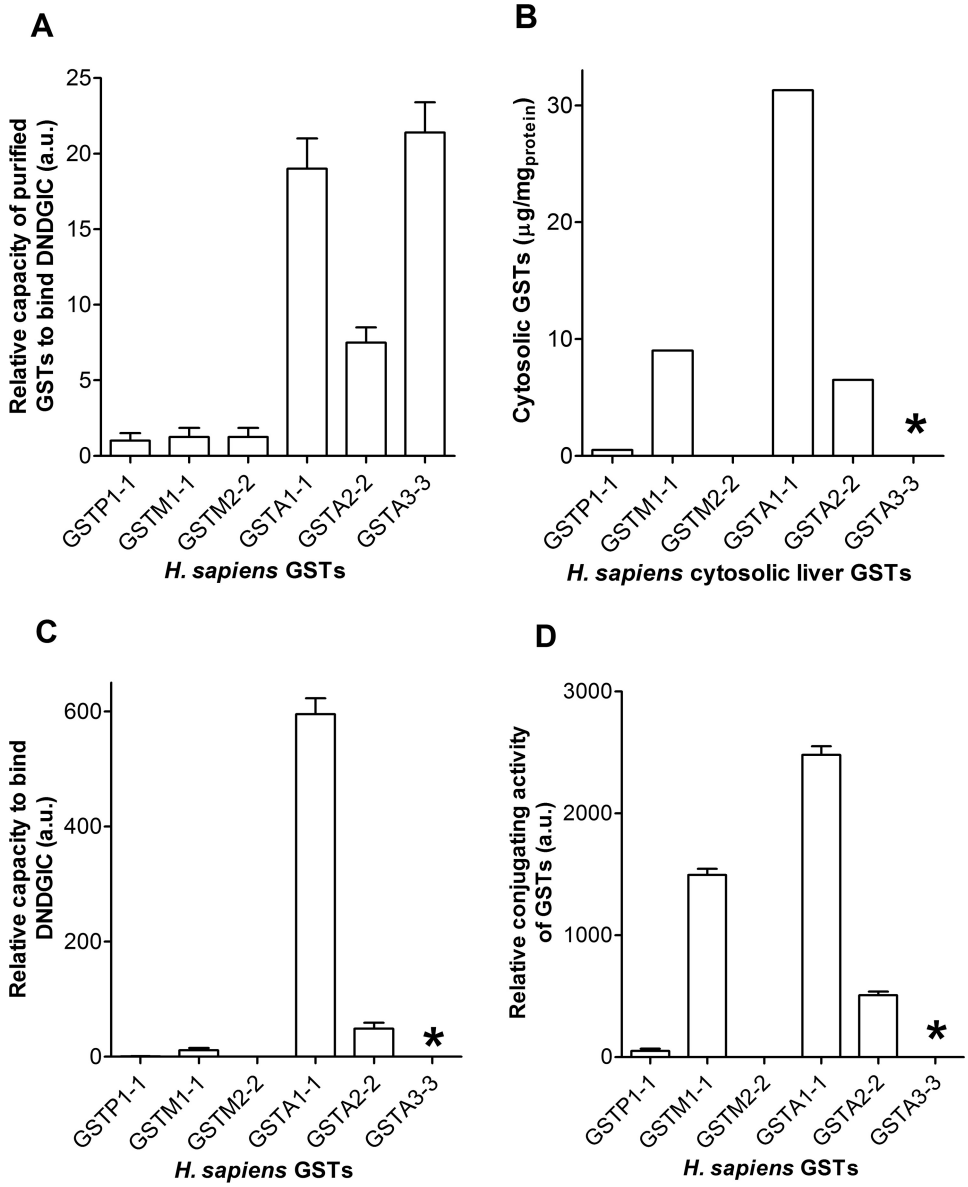

FIGURE 9. ***In vitro* and *in vivo* capacity of human hepatocyte GSTs to bind DNDGIC or to inactivate toxins by conjugation with GSH.** *A*, relative capacity of identical amounts of purified GSTs to bind DNDGIC (data coming from dissociation constant K_{D1} reported in Bocedi *et al.* (23). *a.u.*, arbitrary units. *B*, relative expression of GST variants (microgram of GSTs/mg total protein) in human hepatocytes (from Ref. 58). *C*, relative capacity of human GSTs to bind DNDGIC in hepatocytes (relative concentrations of GST variants in liver (58) × their corresponding affinities for DNDGIC reported in *panel A*). *D*, relative capacity of human GSTs in hepatocytes to conjugate GSH to toxic electrophilic compounds (relative concentrations of GST variants (58) × their corresponding specific activities toward CDNB (units/mg = 80 for A1-1, 166 for M1-1 (59), 78 for A2-2, 157 for M1-1, 182 for M2-2, and 129 for P1-1 (60)). *Error bars* are S.E. *, the null contribution of GSTA3-3 in the liver cell protection is simply due to its absence from these cells (30), as shown in *panel B*.

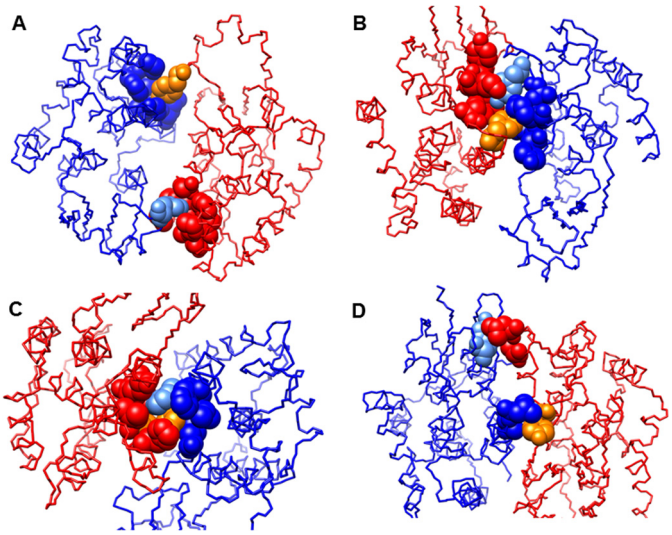

FIGURE 10. **Structural requirements for cooperative interactions in GSTs.** *A*, the lock-and-key motif in *h*GSTP1-1. Tyr-49 (Tyr50 with Met-1 residue) is reported in corn blue for chain A and in *orange* for chain B. Met-91, Val-92, Gly-95, Pro-128, Phe-129, and Leu-132 in chain A and B are reported as *blue* and *red spheres*, respectively. *B*, the "alternative" motif found in GST from *S. haematobium*. Tyr-92 of the two subunits is reported in *corn blue* for chain A and in *orange* for chain B; Arg-76, Tyr-77, Lys-80, and Met-85 in chain A and B are reported as *blue* and *red spheres*, respectively. *C*, the clasp motif found in GSTD4-4 from *A. dirus*. Phe-104 of the two subunits is reported in *corn blue* for chain A and in *orange* for chain B; Arg-67, His-100, Leu-103, and Val-107 in chain A and B are reported as *blue* and *red spheres*, respectively. *D*, the alternative motif of the *h*GSTT2-2. Tyr-73 of the two subunits are reported in *corn blue* for chain A and in *orange* for chain B; Leu-89 and Ala-93 in chains A and B are reported as *blue* and *red spheres*, respectively. In all structures the backbone chains are in *blue* and *red* colors.

Schistosoma haematobium GST, which also shows a relevant negative cooperativity ($n_H = 0.65$), lacks this specific motif but shows an alternative insertion of an aromatic residue (Tyr-92) into a hydrophobic cavity of the adjacent subunit formed by Lys-80 and Met-85 but also surrounded by the Arg-76 and Tyr-77 (Fig. 10*B*). In the Ser-GSTs, a lock-and-key motif is always present but different from that reported in mammalian Alpha/Mu/Pi classes. A striking characteristic of this motif involving the "key" residue is that it not only inserts into a hydrophobic pocket of the neighboring subunit but also itself acts as part of the lock for the other subunit key. In addition, the key residues from both subunits hook around each other in an aromatic pi-pi interaction, through slightly offset aromatic ring stacking, generating a "clasp" in the middle of the subunit interface (37). The clasp motif is formed by an aromatic residue of Phe-104 of one subunit and the Arg-67, His-100, Leu-103, and Val-107 of the second subunit and vice versa occurs among the Phe-104 of the second subunit and the same four residues of the first subunit. The clasp motif appears like two hands interlocked with the two Phe-104 residues in the central portion (Fig. 10*C*). The human GSTT2-2 lacks this peculiar motif, but similar to the *S. haematobium* GST, an alternative aromatic residue (Tyr-73) is inserted in a hydrophobic cavity of the adjacent subunit formed by Leu-89 and Ala-93 possibly acting as an ancillary transmission device for cooperativity (Fig. 10*D*). In the Cys-GSTs no similar intersubunit connections were observed, in full agreement with the absence of any kinetic or binding cooperativity (Table 1). Obviously, the alternative motifs proposed here for *S. haematobium* GST and for GSTT2-2 are plausible but only hypothetical structural mechanisms that must be confirmed in the future by mutagenesis experiments.

Discussion

Negative cooperativity is even now one of the most intriguing phenomena in biochemistry, but many aspects are still to be explored (38–41). A typical case of negative cooperativity is the half-of-the-sites interaction, *i.e.* when binding of a specific inhibitor to one subunit of a dimeric enzyme results in the adjacent vacant subunit becoming fully inactive (42). Alternatively, the binding of the inhibitor to the first subunit may give the second subunit lower affinity for the same compound. In this case the adjacent subunit retains its original activity even in the presence of an excess of inhibitor (43). In this complex scenario of different and sometimes opposite effects triggered by negative cooperativity mechanisms, a much debated question is the identification of specific physiological functions. Cornish-Bowden stated in 1975 that physiological role of negative cooperativity remained unclear (44), and almost 40 years later he concluded that there had been very little progress in understanding its biological function, although he proposed that negative cooperativity can better be understood in a network context, generating very high sensitivity of metabolite concentrations to flux perturbations (45). The particular cooperativity found in the GST superfamily and described in this paper shows some novelties in this context. The interaction of GSTs with DNDGIC, a toxic compound that can be neutralized by these enzymes but that also represents a strong inhibitor for all GSTs, offers a diverse scenario of utilization of negative cooperativity that spans from a classical half-of-the sites interaction to a cooperative self-preservation. The availability of many purified GST variants and the corresponding X-ray diffraction data offered us an extraordinary investigative strength to define evolutionary pathways and structural requirements for this phenomenon. A first conclusion is that these detoxifying enzymes have evolved to acquire a cooperative self-preservation mechanism that helps to save a residual enzymatic activity in the case of DNDGIC overproduction *i.e.* after NO toxicity. The evolution progress appears evident, observing that all tested Cys-GSTs (the oldest variants close to the ancestral GST), despite their dimeric structures and their three-dimensional shapes similar to the more recently evolved GSTs, display no (or very scarce) trace of negative cooperativity. In addition, most Ser-GSTs, which also appeared after Cys-GSTs but before the Tyr-GSTs in the evolution pathway of GSTs, display a less efficient cooperative self-preservation than that found in the more recently evolved Tyr-GSTs (Tables 1 and 2 and Fig. 2). A structural explanation of these differences has been recognized. The typical lock-and-key motif involving one hydrophobic residue of one subunit, which is inserted between helix 4 and helix 5 of the second one, is only present in the Tyr-GSTs (35) and appears to be the most efficient structural machinery to achieve an optimized self-preservation with n_H values near 0.5, which indicates a very strong negative cooperativity for a dimeric protein (see Table 1). A different but less efficient intersubunit connection, termed clasp motif, has been found in a few Ser-GSTs (37) but not in all. In addition, these connections are not unique; in one Tyr-GST and in one Ser-GST variants other

alternative modalities of communication may be proposed (see Fig. 10, *B* and *D*). Thus it appears that diverse structural motifs have been adopted by GSTs during evolution to reach an efficient intersubunit communication. Conversely, none of the tested bacterial Cys-GSTs, close to the ancestral forms of GSTs, display any similar structural insertions. Interestingly, one of the most efficiently self-protecting GSTs is the GSTP1-1, whose enzymatic activity must definitely be saved, as it is the sole GST variant expressed in some tissues. The half-of-the-sites interaction leading to full inactivation, found for the two GSTs showing the highest propensity to bind DNDGIC, is probably the price to be paid to reach such astonishing affinity. The finding that GSTs with highest affinity (*i.e.* the Alpha class variants) surround in large amounts the nuclear envelope is strong evidence that one primary function of these enzymes is to protect the nucleus and DNA from DNDGIC, leaving to the Mu class GSTs the classic catalytic role against other toxins. We must remember that in all cells Alpha class GSTs are often combined with variable amounts of Mu class GSTs, and then this sacrifice is probably well balanced by the presence of a sufficient potential of active enzyme for the classical conjugation of GSH to other toxins (see Fig. 9). Alternatively, the presence of substantial amounts of GSTA1-2 or GSTA2-3 heterodimers (5) could also guarantee a residual conjugating activity toward electrophilic toxins in the presence of DNDGIC. In fact, this appears as a reasonable explanation for the existence of GST heterodimers.

In conclusion, the cooperative self-preservation found in GSTs, but probably also operative in a number of other multimeric enzymes, may be considered a novel biological application of Le Chatelier's principle: "If there is a change in the condition of a system in equilibrium, the system will adjust itself in such a way as to counteract, as far as possible, the effect of that change" (46). In our case, whenever a chemical factor (for example DNDGIC) perturbs or inhibits the enzyme, it opposes this perturbation by developing some negative cooperativity that tends to relieve that stress.

Other Enzymes Have Acquired Cooperative Self-preservation—Many studies describing the interaction of specific inhibitors to homo-multimeric enzymes have revealed that biphasic inhibition patterns are not an unusual finding. This suggests that negative cooperativity mechanisms could have been adopted and perfected to achieve self-preservation, but curiously this possibility has only rarely been taken into consideration. An extended examination of the scientific literature now leads to the realization that 100s of enzymes display this behavior. For example, aminoglycoside *N*-acetyltransferase (47), adenylosuccinate lyase (48), adenylosuccinate synthetase (49), enoyl-ACP reductase (50), thymidylate synthase (51), pyruvate kinase (43), formate dehydrogenase (52), and pyruvate phosphate dikinase (53) show negative cooperativity toward specific inhibitors, but no allusion to a possible self-preservation function has been made. Conversely, the study of the prolidase inhibition by the natural inhibitor phosphoenolpyruvate represents a rare example of a discovered negative cooperativity explicitly indicated as "an expedient evolutionary solution to the problem of eluding an endogenous inhibitor" (54).

Our intention in this paper has been to draw attention and analyze a role for negative cooperativity that has been given almost no attention in the past. However, we do not suggest that self-preservation is the only reason why it should have been selected in evolution. In other cases increasing the sensitivity of the concentrations of intermediate metabolites (45) may provide a better explanation, although it does not seem to apply to the glutathione transferases.

Experimental Procedures

Purified GSTs—Human GSTP1-1, human GSTA1-1, human GSTA2-2, human GSTA3-3, human GSTM2-2, *O. volvulus* GST2, *S. haematobium* GST, *L. cuprina* GSTc, *Anopheles dirus* GSTD3-3, *A. dirus* GSTD4-4, *A. dirus* GSTD5-5, human GSTT2-2, *Ochrobactrum anthropi* GST, *Burkholderia xenovorans* GST, *Sphingomonas paucimobilis* GST, and *Proteus mirabilis* GST, all except *L. cuprina* GST (M. W. Parker, personal gift), were expressed and purified as described previously (23).

Synthesis of Dinitrosyl-diglutathionyl Iron Complex—DNDGIC was prepared essentially as described previously (55). Briefly, 1 ml of 0.5 mM $FeSO_4$ (dissolved in degassed water to avoid rapid oxidation to the ferric state) was added to 10 ml (final volume) of 0.1 mM potassium phosphate buffer, pH 7.4, containing 20 mM GSH and 2 mM S-nitrosoglutathione (25 °C). After 10 min the reaction was almost complete, and the resulting stock solution of DNDGIC (50 μM) was stable for at least 3 h. More concentrated solutions (up to 1 mM DNDGIC) were also obtained by incubating GSH 20 mM, 4 mM S-nitrosoglutathione, and variable $FeSO_4$ (up to 1 mM) in 0.05 M sodium borate buffer, pH 11.0.

Inhibition by DNDGIC—The interaction of the inhibitor DNDGIC with Tyr-GSTs and Ser-GSTs has been studied by means of inhibition experiments using the classical enzymatic reaction, *i.e.* GSH (0.1 mM), 1-chloro-2,4-dinitrobenzene (1 mM) in 0.1 M potassium phosphate buffer and variable additions of DNDGIC. The spectrophotometric procedure was identical to the one described previously (23). Inhibition kinetics data were fitted by a two site inhibition Equation 1,

$$Y = \frac{B_{max1}[\text{DNDGIC}]}{K_{i1}^{app} + [\text{DNDGIC}]} + \frac{B_{max2}[\text{DNDGIC}]}{K_{i2}^{app} + [\text{DNDGIC}]} \qquad \text{(Eq. 1)}$$

where Y is the percent of inhibition, and $B_{max1} + B_{max2} = 100$.

K_{i1}^{app} and K_{i2}^{app} are the apparent values from which the true inhibition constants are calculated via $K_{i1}^{app} = K_{i1}(1 + [GSH]/K_m)$, and $K_{i2}^{app} = K_{i2}(1 + [GSH]/K_m)$ and the K_m values derived from Ref. 23.

Fluorescence Experiments—Quenching of intrinsic fluorescence by DNDGIC was measured in a single photon counting spectrofluorometer (Fluoromax, S.A. Instruments, Paris, France) with a sample holder thermostated at 25 °C (37 °C for GSTT2-2). Excitation was at 280 nm, and emission was at 340 nm. In a typical experiment GST (2 μM) was incubated with variable amounts of DNDGIC (from 0.2 to 20 μM) in 1 ml of 0.1 M potassium phosphate buffer, pH 7.4. After 5 min (40 min for GSTT2-2), the fluorescence at 340 nm was measured and corrected for inner filter effect. Data were fitted by a two-site binding equation,

$$Y = \frac{B_{max1}[\text{DNDGIC}]}{K_{D1} + [\text{DNDGIC}]} + \frac{B_{max2}[\text{DNDGIC}]}{K_{D2} + [\text{DNDGIC}]} \quad \text{(Eq. 2)}$$

where Y is the percent of fluorescence quenching and $B_{max1} + B_{max2} = 100$.

As shown in Tables 1 and 2, K_D values are very similar to those for K_i obtained by kinetic experiments, except for GSTA1-1 and GSTA3-3, which display half-site interaction (full inhibition in the half-saturated enzyme with DNDGIC) but two distinct binding constants.

Hill Plot and Hill Coefficients—Hill coefficients (n_H) were calculated by fitting fluorometric or inhibition data to the equation,

$$Y = Y_{max}\frac{[\text{DNDGIC}]^{n_H}}{K_i^{n_H} + [\text{DNDGIC}]^{n_H}} \quad \text{(Eq. 3)}$$

where Y is the percent of inhibition or fluorescence perturbation, and n_H is the Hill coefficient.

Visualization of negative cooperativity (or its absence) was also obtained by means of the Hill plot (Equation 4),

$$\log\left(\frac{Y}{100 - Y}\right) = n_H \log[\text{DNDGIC}] - \log K_1 \quad \text{(Eq. 4)}$$

where Y is percent of inhibition or percent of fluorescence quenching.

GST Activity—GST activity was assayed by incubating 0.1 mM GSH and 1 mM CDNB in 0.1 M potassium phosphate buffer, pH 6.5 (25 °C). The reaction was followed spectrophotometrically at 340 nm, where the CDNB-GSH adduct absorbs (ϵ = 9600 M^{-1} cm^{-1}).

Structural Studies—Illustrations of X-ray structures were created by UCSF Chimera (56). PDB ID used to identify interface connectivities were: *h*GSTP1-1, 6GSS; hGSTA1-1, 1K3L; *h*GSTA2-2, 2WJU; *h*GSTA3-3, 1TDI; *h*GSTM2-2, 2AB6; *O. volvulus* GST2, 1TU8; *S. haematobium* GST, 1OE7; *L. cuprina* GSTc (Parker, personal communication); *A. dirus* GSTD3-3, 1JLV; *A. dirus* GSTD4-4, 3F63; *A. dirus* GSTD5-5, 1R5A; *h*GSTT2-2, 3LJR; *O. anthropi* GST, 2NTO; *B. xenovorans* GST, 2DSA; *S. paucimobilis* GST, 1F2E; *P. mirabilis* GST, 2PMT. Finally, *h*GSTP1-1 with DNGIC was derived from PDB ID 1ZGN.

The residue numbering of all these GSTs is those reported in the Protein Data Bank. In this library only human GSTP1-1, GSTA1-1, and GSTM2-2 sequences do not display Met-1.

Statistical Data Analysis—Kinetic and thermodynamic data were analyzed and displayed by GraphPad Prism software (La Jolla, CA). The experimental values reported in Table 1 and Table 2 and in Figs. 3–7 are the means of three independent experiments ± S.D. The propagation of uncertainties for the quotients in Tables 1 and 2 were analyzed according to the classical statistical methods (57).

Author Contributions—A. B. conducted most of the experiments and analyzed the results. R. F. conducted some kinetic experiments. M. L. B., A. M. C., and G. F. collaborated to logic development of the paper. A. C.-B. and B. M. collaborated in the writing of the paper and in critically evaluating the cooperativity data. G. R. conceived the idea for the project and wrote the paper.

Acknowledgment—We thank Prof. J. Z. Pedersen for helpful discussion of the results.

References

1. Armstrong, R. N. (1997) Structure, catalytic mechanism, and evolution of the glutathione transferases. *Chem. Res. Toxicol.* **10,** 2–18
2. Hayes, J. D., Flanagan, J. U., and Jowsey, I. R. (2005) Glutathione transferases. *Annu. Rev. Pharmacol. Toxicol.* **45,** 51–88
3. Rinaldi, R., Eliasson, E., Swedmark, S., and Morgenstern, R. (2002) Reactive intermediates and the dynamics of glutathione transferases. *Drug Metab. Dispos.* **30,** 1053–1058
4. Eaton, D. L., and Bammler, T. K. (1999) Concise review of the glutathione *S*-transferases and their significance to toxicology. *Toxicol. Sci.* **49,** 156–164
5. Mannervik, B., and Jensson, H. (1982) Binary combinations of four protein subunits with different catalytic specificities explain the relationship between six basic glutathione *S*-transferases in rat liver cytosol. *J. Biol. Chem.* **257,** 9909–9912
6. Jakobson, I., Warholm, M., and Mannervik, B. (1979) The Binding of a substrate and a product of the enzymatic reaction to glutathione *S*-transferase. *J. Biol. Chem.* **254,** 7085–7089
7. Danielson, U. H., and Mannervik, B. (1985) Kinetic independence of the subunits of cytosolic glutathione transferase from the rat. *Biochem. J.* **231,** 263–267
8. Tahir, M. K., and Mannervik, B. (1986) Simple inhibition studies for distinction between homodimeric and heterodimeric isoenzymes of glutathione transferase, *J. Biol. Chem.* **261,** 1048–1051
9. Ricci, G., Lo Bello, M., Caccurri, A. M., Pastore, A., Nuccetelli, M., Parker, M. W., and Federici, G. (1995) Site-directed mutagenesis of human glutathione transferase P1-1: mutation of Cys-47 induces a positive cooperativity in glutathione transferase P1-1. *J. Biol. Chem.* **270,** 1243–1248
10. Lo Bello, M., Nuccetelli, M., Chiessi, E., Lahm, A., Mazzetti, A. P., Battistoni, A., Caccuri, A. M., Oakley, A. J., Parker, M. W., Tramontano, A., Federici, G., and Ricci, G. (1998) Mutations of Gly to Ala in human glutathione transferase P1-1 affect helix 2 (G-site) and induce positive cooperativity in the binding of glutathione. *J. Mol. Biol.* **284,** 1717–1725
11. Lo Bello, M., Battistoni, A., Mazzetti, A. P., Board, P. G., Muramatsu, M., Federici, G., and Ricci, G. (1995) Site-directed mutagenesis of human glutathione transferase P1-1. Spectral, kinetic, and structural properties of Cys-47 and Lys-54 mutants. *J. Biol. Chem.* **270,** 1249–1253
12. Hegazy, U. M., Mannervik, B., and Stenberg, G. (2004) Functional role of the lock and key motif at the subunit interface of glutathione transferase P1-1. *J. Biol. Chem.* **279,** 9586–9596
13. Vararattanavech, A., and Ketterman, A. (2003) Multiple roles of glutathione binding-site residues of glutathione *S*-transferase. *Protein Pept. Lett.* **10,** 441–448
14. Labrou, N. E., Mello, L. V., and Clonis, Y. D. (2001) The conserved Asn49 of maize glutathione *S*-transferase I modulates substrate binding, catalysis and intersubunit communication. *Eur. J. Biochem.* **268,** 3950–3957
15. Ricci, G., Del Boccio, G., Pennelli, A., Aceto, A., Whitehead, E. P., and Federici, G. (1989) Nonequivalence of the two subunits of horse erythrocyte glutathione transferase in their reaction with sulfhydryl reagents. *J. Biol. Chem.* **264,** 5462–5467
16. Reinemer, P., Dirr, H. W., Ladenstein, R., Huber, R., Lo Bello, M., Federici, G., and Parker, M. W. (1992) Three-dimensional structure of class pi glutathione *S*-transferase from human placenta in complex with *S*-hexylglutathione at 2.8 Å resolution. *J. Mol. Biol.* **227,** 214–226
17. Ricci, G., Caccuri, A. M., Lo Bello, M., Parker, M. W., Nuccetelli, M., Turella, P., Stella, L., Di Iorio, E. E., and Federici, G. (2003) Glutathione transferase P1-1: self-preservation of an anti-cancer enzyme. *Biochem. J.* **376,** 71–76
18. Xiao, B., Singh, S. P., Nanduri, B., Awasthi, Y. C., Zimniak, P., and Ji, X. (1999) Crystal structure of a murine glutathione *S*-transferase in complex with a glutathione conjugate of 4-hydroxynon-2-enal in one subunit and glutathione in the other: evidence of signaling across the dimer interface. *Biochemistry* **38,** 11887–11894

19. Lien, S., Gustafsson, A., Andersson, A.-K., and Mannervik, B. (2001) Human glutathione transferase A1-1 demonstrates both half-of-the-sites and all-of-the-sites reactivity. *J. Biol. Chem.* **276,** 35599–35605
20. Liebau, E., De Maria, F., Burmeister, C., Perbandt, M., Turella, P., Antonini, G., Federici, G., Giansanti, F., Stella, L., Lo Bello, M., Caccuri, A. M., and Ricci, G. (2005) Cooperativity and pseudo-cooperativity in the glutathione *S*-transferase from. *Plasmodium falciparum*. *J. Biol. Chem.* **280,** 26121–26128
21. Liebau, E., Dawood, K. F., Fabrini, R., Fischer-Riepe, L., Perbandt, M., Stella, L., Pedersen, J. Z., Bocedi, A., Petrarca, P., Federici, G., and Ricci, G. (2009) Tetramerization and cooperativity in *Plasmodium falciparum* glutathione *S*-transferase are mediated by atypic loop 113–119. *J. Biol. Chem.* **284,** 22133–22139
22. Caccuri, A. M., Antonini, G., Ascenzi, P., Nicotra, M., Nuccetelli, M., Mazzetti, A. P., Federici, G., Lo Bello, M., and Ricci, G. (1999) Temperature adaptation of glutathione *S*-transferase P1-1. A case for homotropic regulation of substrate binding. *J. Biol. Chem.* **274,** 19276–19280
23. Bocedi, A., Fabrini, R., Farrotti, A., Stella, L., Ketterman, A. J., Pedersen, J. Z., Allocati, N., Lau, P. C., Grosse, S., Eltis, L. D., Ruzzini, A., Edwards, T. E., Morici, L., Del Grosso, E., Guidoni, L., Bovi, D., *et al.* (2013) The impact of nitric oxide toxicity on the evolution of the glutathione transferase superfamily: a proposal for an evolutionary driving force. *J. Biol. Chem.* **288,** 24936–24947
24. Lobysheva, I. I., Stupakova, M. V., Mikoyan, V. D., Vasilieva, S. V., and Vanin, A. F. (1999) Induction of the SOS DNA repair response in *Escherichia coli* by nitric oxide donating agents: dinitrosyl iron complexes with thiol-containing ligands and *S*-nitrosothiols. *FEBS Lett.* **454,** 177–180
25. Vasilieva, S. V., Moshkovskaya, E. Y., Sanina, N. A., Aldoshin, S. M., and Vanin, A. F. (2004) Genetic signal transduction by nitrosyl iron complexes in *Escherichia coli*. *Biochemistry* **69,** 883–889
26. Boese, M., Keese, M. A., Becker, K., Busse, R., and Mülsch, A. (1997) Inhibition of glutathione reductase by dinitrosyl-iron-dithiolate complex. *J. Biol. Chem.* **272,** 21767–21773
27. Cesareo, E., Parker, L. J., Pedersen, J. Z., Nuccetelli, M., Mazzetti, A. P., Pastore, A., Federici, G., Caccuri, A. M., Ricci, G., Adams, J. J., Parker, M. W., and Lo Bello, M. (2005) Nitrosylation of human glutathione transferase P1-1 with dinitrosyl diglutathionyl iron complex *in vitro* and *in vivo*. *J. Biol. Chem.* **280,** 42172–42180
28. Abeliovich, H. (2005) An empirical extremum principle for the Hill coefficient in ligand-protein interactions showing negative cooperativity. *Biophys. J.* **89,** 76–79
29. De Maria, F., Pedersen, J. Z., Caccuri, A. M., Antonini, G., Turella, P., Stella, L., Lo Bello, M., Federici, G., and Ricci, G. (2003) The specific interaction of dinitrosyl-diglutathionyl-iron complex, a natural NO carrier, with the glutathione transferase superfamily: suggestion for an evolutionary pressure in the direction of the storage of nitric oxide. *J. Biol. Chem.* **278,** 42283–42293
30. Larsson, E., Mannervik, B., and Raffalli-Mathieu, F. (2011) Quantitative and selective PCR analysis of highly similar human Alpha-class glutathione transferases. *Anal. Biochem.* **412,** 96–101
31. Stella, L., Pallottini, V., Moreno, S., Leoni, S., De Maria, F., Turella, P., Federici, G., Fabrini, R., Dawood, K. F., Bello, M. L., Pedersen, J. Z., and Ricci, G. (2007) Electrostatic association of glutathione transferase to the nuclear membrane: evidence of an enzyme defense barrier at the nuclear envelope. *J. Biol. Chem.* **282,** 6372–6379
32. Fabrini, R., Bocedi, A., Pallottini, V., Canuti, L., De Canio, M., Urbani, A., Marzano, V., Cornetta, T., Stano, P., Giovanetti, A., Stella, L., Canini, A., Federici, G., and Ricci, G. (2010) Nuclear shield: a multi-enzyme taskforce for nucleus protection. *PLoS ONE* **5,** e14125
33. Hegazy, U. M., Musdal, Y., and Mannervik, B. (2013) Hidden allostery in human glutathione transferase P1-1 unveiled by unnatural amino acid substitutions and inhibition studies. *J. Mol. Biol.* **425,** 1509–1514
34. Stenberg, G., Abdalla, A.-M., and Mannervik, B. (2000) Tyrosine 50 at the subunit interface of dimeric human glutathione transferase P1-1 is a structural key residue for modulating protein stability and catalytic function. *Biochem. Biophys. Res. Commun.* **271,** 59–63
35. Sayed, Y., Wallace, L. A., and Dirr, H. W. (2000) The hydrophobic lock-and-key intersubunit motif of glutathione transferase A1-1: implications for catalysis, ligandin function, and stability. *FEBS Lett.* **465,** 169–172
36. Hornby, J. A., Codreanu, S. G., Armstrong, R. N., and Dirr, H. W. (2002) Molecular recognition at the dimer interface of a class Mu glutathione transferase: role of a hydrophobic interaction motif in dimer stability and protein function. *Biochemistry* **41,** 14238–14247
37. Wongsantichon, J., and Ketterman, A. J. (2006) An intersubunit lock-and-key "clasp" motif in the dimer interface of Delta class glutathione transferase. *Biochem. J.* **394,** 135–144
38. Cornish-Bowden, A. (2014) Understanding allosteric and cooperative interactions in enzymes. *FEBS J.* **281,** 621–632
39. Conway, A., and Koshland, D. E., Jr. (1968) Negative cooperativity in enzyme action. Binding of diphosphopyridine nucleotide to glyceraldehyde-3-phosphate dehydrogenase. *Biochemistry* **7,** 4011–4023
40. Koshland, D. E., Jr. (1996) The structural basis of negative cooperativity: receptors and enzymes. *Curr. Opin. Struct. Biol.* **6,** 757–761
41. Monod, J., Wyman, J., and Changeux, J.-P. (1965) On the nature of allosteric transitions: a plausible model. *J. Mol. Biol.* **12,** 88–118
42. Herzfeld, J., Ichiye, T., and Jung, D. (1981) Molecular symmetry and metastable states of enzymes exhibiting half-of-the-sites reactivity. *Biochemistry* **20,** 4936–4941
43. Tomich, J. M., Marti, C., and Colman, R. F. (1981) Modification of two essential cysteines in rabbit muscle pyruvate kinase by the guanine nucleotide analogue 5′-[*p*-(fluorosulfonyl)benzoyl]guanosine. *Biochemistry* **20,** 6711–6720
44. Cornish-Bowden, A. (1975) The physiological significance of negative cooperativity. *J. Theor. Biol.* **51,** 233–235
45. Cornish-Bowden, A. (2013) The physiological significance of negative cooperativity revisited. *J. Theor. Biol.* **319,** 144–147
46. Laidler, K. J., and Meiser, J. H. (1999) *Physical Chemistry*, p.169, Houghton Mifflin Co., Boston
47. Magnet, S., Lambert, T., Courvalin, P., and Blanchard, J. S. (2001) Kinetic and mutagenic characterization of the chromosomally encoded *Salmonella enterica* AAC(6′)-Iy aminoglycoside *N*-acetyltransferase. *Biochemistry* **40,** 3700–3709
48. Gite, S. U., and Colman, R. F. (1996) Affinity labeling of the active site of rabbit muscle adenylosuccinate lyase by 2-[(4-bromo-2,3-dioxobutyl) thio]adenosine 5′-monophosphate. *Biochemistry* **35,** 2658–2667
49. Lee, P., Gorrell, A., Fromm, H. J., and Colman, R. F. (1999) Implication of arginine-131 and arginine-303 in the substrate site of adenylosuccinate synthetase of *Escherichia coli* by affinity labeling with 6-(4-bromo-2,3-dioxobutyl)thioadenosine 5′-monophosphate. *Biochemistry* **38,** 5754–5763
50. Protasevich, I. I., Brouillette, C. G., Snow, M. E., Dunham, S., Rubin, J. R., Gogliotti, R., and Siegel, K. (2004) Role of inhibitor aliphatic chain in the thermodynamics of inhibitor binding to *Escherichia coli* enoyl-ACP reductase and the Phe203Leu mutant: a proposed mechanism for drug resistance. *Biochemistry* **43,** 13380–13389
51. Reilly, R. T., Barbour, K. W., Dunlap, R. B., and Berger, F. G. (1995) Biphasic binding of 5-fluoro-2′-deoxyuridylate to human thymidylate synthase. *Mol. Pharmacol.* **48,** 72–79
52. Labrou, N. E., Rigden, D. J., and Clonis, Y. D. (2000) Characterization of the NAD+ binding site of *Candida boidinii* formate dehydrogenase by affinity labelling and site-directed mutagenesis. *Eur. J. Biochem.* **267,** 6657–6664
53. Evans, C. T., Goss, N. H., and Wood, H. G. (1980) Pyruvate phosphate dikinase: affinity labeling of the adenosine 5′-triphosphate-adenosine 5′-monophosphate site. *Biochemistry* **19,** 5809–5814
54. Mock, W. L., and Liu, Y. (1995) Inhibition of prolidase by phosphoenolpyruvate is biphasic: avoidance of endogenous-metabolite inactivation by cooperativity within an enzyme dimer. *Bioorg. Med. Chem. Lett.* **5,** 627–630
55. Lo Bello, M., Nuccetelli, M., Caccuri, A. M., Stella, L., Parker, M. W., Rossjohn, J., McKinstry, W. J., Mozzi, A. F., Federici, G., Polizio, F., Pedersen, J. Z., and Ricci, G. (2001) Human glutathione transferase P1-1 and nitric oxide carriers: a new role for an old enzyme. *J. Biol. Chem.* **276,** 42138–42145

56. Pettersen, E. F., Goddard, T. D., Huang, C. C., Couch, G. S., Greenblatt, D. M., Meng, E. C., and Ferrin, T. E. (2004) UCSF Chimera: a visualization system for exploratory research and analysis. *J. Comput. Chem.* **25,** 1605–1612
57. Taylor, J. R. (1997) *An Introduction to Error Analysis,* 2nd Ed., pp. 45–79, University Science Books, Sausalito, CA
58. Rowe, J. D., Nieves, E., and Listowsky, I. (1997) Subunit diversity and tissue distribution of human glutathione *S*-transferases: interpretations based on electrospray ionization-MS and peptide sequence-specific antisera. *Biochem. J.* **325,** 481–486
59. Paumi, C. M., Smitherman, P. K., Townsend, A. J., and Morrow, C. S. (2004) Glutathione *S*-transferases (GSTs) inhibit transcriptional activation by the peroxisomal proliferator-activated receptor γ (PPAR γ) ligand, 15-deoxy-δ-12,14prostaglandin J2 (15-d-PGJ2). *Biochemistry* **43,** 2345–2352
60. Hayeshi, R., Mutingwende, I., Mavengere, W., Masiyanise, V., and Mukanganyama, S. (2007) The inhibition of human glutathione *S*-transferases activity by plant polyphenolic compounds ellagic acid and curcumin. *Food Chem. Toxicol.* **45,** 286–295